IAC-09-A1.4.09

Probabilistic Assessment of Radiation Risk for Astronauts in Space Missions

Myung-Hee Y. Kim
Universities Space Research Association, Houston, TX 77058, USA
myung-hee.y.kim@nasa.gov

Giovanni De Angelis
Instituto Superiore di Sanita, Rome, Italy
giovanni.deangelis@iss.it

Francis A. Cucinotta
NASA Johnson Space Center, Houston, TX 77058, USA
francis.a.cucinotta@nasa.gov

ABSTRACT

Accurate estimations of the health risks to astronauts due to space radiation exposure are necessary for future lunar and Mars missions. Space radiation consists of solar particle events (SPEs), comprised largely of medium energy protons (less than several hundred MeV); and galactic cosmic rays (GCR), which include high energy protons and heavy ions. While the frequency distribution of SPEs depends strongly upon the phase within the solar activity cycle, the individual SPE occurrences themselves are random in nature. A solar modulation model has been developed for the temporal characterization of the GCR environment, which is represented by the deceleration potential, ϕ. The risk of radiation exposure to hardware as well as to astronauts from SPEs during extra-vehicular activities (EVAs) or in lightly shielded vehicles is a major concern for radiation protection. To support the probabilistic risk assessment for EVAs, which could be up to 15% of crew time on lunar missions, we estimated the probability of SPE occurrence as a function of solar cycle phase using a non-homogeneous Poisson model to fit the historical database of measurements of protons with energy > 30 MeV, Φ_{30}. The resultant organ doses and dose equivalents, as well as effective whole body doses, for acute and cancer risk estimations are analyzed for a conceptual habitat module and for a lunar rover during space missions of defined durations. This probabilistic approach to radiation risk assessment from SPE and GCR is in support of mission design and operational planning for future manned space exploration missions.

1. Introduction

Space radiation is a concern for astronaut's health and safety, including risks of cancer, acute radiation sickness, and degenerative risks (Cucinotta and Durante 2006; Durante and Cucinotta 2008). The galactic cosmic ray (GCR) environment varies by about 2-fold in intensity over the approximately 11-year solar cycle. Crew return vehicle design and dose limit constraints implemented by NASA (NCRP, 2000; Cucinotta and Durante, 2006), necessitate prediction of the long-term behavior of solar cycle activity for future projections of radiation dose to astronauts onboard the International Space Station (ISS) and on missions to the moon and Mars. Solar cycle forecasting, even using the sophisticated methods discussed by Withbroe (1989) is not sufficiently accurate, due to the lack of quantitative theories for solar activity cycles. A statistical model was developed as an analysis tool using the accumulated sunspot data for the numbered cycles for the years 1750 through the one most recently completed (Kim and Wilson, 2000; Kim et al. 2004; Kim et al. 2006; Wilson et al. 1999). Because the solar activity cycle affects the near Earth environment, a correlated quantity of the ground-based neutron monitor rate was estimated from the resultant projection of sunspot number into the near future. The quantity of interest for radiation protection, the GCR deceleration potential ϕ has been calculated using the estimated neutron monitor rate. The GCR radiation environment was estimated as a function of ϕ by using GCR predictive models (Badhwar and O'Neill, 1992; Badhwar et al. 1994; Lopate and Simpson, 1991; Nymmik et al. 1996; O'Neill, 2006; Wilson et al. 1999).

Solar particle events (SPEs) occur quite often, and it is difficult to predict their onset and size. Most SPEs would lead to small crew doses even for light spacecraft or EVA shielding, and only a small proportion (about 10%) of events lead to significant organ doses of >10 mGy-Eq. However, many small

events can disrupt or delay mission operations leading to excessive costs. For space missions with longer duration, multiple exposures to SPEs with intense particle fluxes and high energy levels are the major concern. Although the risk of early effects may be small due to the reduction of dose-rates behind shielding (Hu et al. 2009), there remains a significant cancer risk for some events (Cucinotta 1999; Cucinotta and Durante 2006; Durante and Cucinotta 2008). A record of occurrence times and proton fluence levels >30 MeV, Φ_{30}, for 370 events was gathered over 5 solar cycles, spanning the years 1954 to present. From the analysis of SPEs over the past 5 solar cycles, the association between SPE occurrence and solar activity has been studied, but without recognizable pattern in each of the solar cycles (Goswami et al. 1988; Kim et al. 2005; Kim et al. 2006).

For the planning of a worst-case scenario of staying on the moon or Mars, a probability distribution function for SPE occurrence was formed from the available database of SPE proton fluence measurements. The cumulative probabilities of SPEs during short-period missions were defined using the proton fluences of the continuous SPE database (Kim et al. 2007). The random behavior of SPE occurrences was examined using a probabilistic approach in order to insure crew protection and planning of future lunar and Mars stays (Kim et al. 2009a). The number of SPEs in a given window of time was treated as a non-homogeneous Poisson distribution with mean depending on the end points of the window. In addition, the mean number of proton events of a given threshold event size with energy exceeding 30 MeV over some arbitrary time window was estimated for a future non-specific solar cycle. The derivative of this mean was modeled as a parametric function of time within the cycle, and the mean for a particular window was estimated by making use of all the SPE data, including those outside the window of interest. This model-based estimate was considerably more accurate than one based on simple counting of historical events within the window, and a goodness-of-fit test verified that the model indeed provided a reasonable representation of the SPE data in the space era (Kim et al. 2009a). From the prediction of the mean number of SPEs with integral fluence (Φ_{30}) exceeding given thresholds, the cumulative probabilities of SPE frequencies and total proton fluences at various percentiles during a given mission period were defined (Kim et al. 2009a).

For the radiation risk analysis, analytic representations of energy spectra of large events extending over broad energy ranges out to 1 GeV were fitted by Weibull-distributions to the proton fluence measurements (Kim et al. 2007). The defined differential energy spectra of SPE and GCR were propagated through spacecraft and body tissue to specified body organs by using NASA's space radiation transport models, BRYNTRN (Cucinotta et al. 1994; Wilson et al. 1989) for SPE, and HZETRN (Wilson et al. 1991,1995) with QMSFRG database (Cucinotta et al. 2006) for GCR, respectively.

We analyzed blood forming organ (BFO) doses for the comparison of the shielding effectiveness of aluminum and polyethylene for exposure to historically large SPEs; and we estimated organ doses and dose equivalents inside a spherical spacecraft of 5 g/cm^2 aluminum for 30-month Mars mission from GCR at solar minimum. Contributions of different charge groups, overall projectile, and target fragmentation were described; and we compared those with the preliminary dose limits to examine the possibility of detrimental effects. With the consideration of detailed shielding properties provided by a conceptual lunar habitat model, the probabilistic assessment of radiation cancer risk, which is dependent on age, gender, and solar modulation, was calculated at the upper 95% confidence interval (CI) for a 1-yr lunar mission. For the optimization of shield mass and dose reduction during EVA on the lunar surface, radiation analyses were made for conceptual lunar rover configurations. Using the risk mitigation method for candidate spacecraft designs, the proper shielding requirements for crew members can be identified for future exploration mission scenarios.

2. Observed space quantities for statistical models

The official monthly averaged sunspot number (formerly the Zurich sunspot number), which is provided by the Sunspot Index Data Center, Observatoire Royal de Belgique, in Brussels, was obtained from the National Geophysical Data Center (NGDC), U.S. Dept. of Commerce, NOAA, Boulder, CO, for the years 1750 through the present, and categorized into odd and even cycles. There is no immediately obvious pattern in the cycles other than a variation of the 10- to 13-year cycle period. The cycles exhibit fluctuating amplitudes, differing minima and maxima, and variable shapes.

The cosmic ray data from neutron monitors at the Deep River neutron monitor site (longitude 46° N, latitude 77° W, 145-m altitude, and cutoff rigidity of 1.02 GV) were obtained from NGDC for the measurement starting January 1958 to December 1994, which covers cycles from the second half of cycle 19 through 22. There appears to be a reasonably well-established pattern of count rates and

sunspot numbers, even though cycle 20 is nearly independent due to the halt of the declining phase in years of 1971 and 1972. However, clear differences between odd and even cycles have been shown in the relationship between count rates and sunspot numbers.

All available proton flux and fluence data of solar particle events (SPEs) for solar cycles 19-21 (1955-1986) were assembled in the form of a continuous database (Shea and Smart, 1990). From 1986 to 2007 (solar cycles 22 and 23), a SPE list and the GOES spacecraft measurements of the 5-minute average integral proton flux were obtained directly from NGDC. The SPE event-sizes of proton fluences > 30 MeV (Φ_{30}) for solar cycles 19-21 were taken from the Shea and Smart (1990), and those for solar cycles 22 and 23 were calculated using the extensive direct GOES satellite particle measurements of integral proton fluxes. Between the years 1561 and 1950, 71 SPEs with $\Phi_{30} > 2\times10^9$ protons cm^{-2} (McCracken et al. 2001) were also identified from impulsive nitrate enhancements in polar ice cores.

3. Space radiation environment projections using statistical models

3.1 GCR deceleration parameter projection using a solar cycle statistical model

The solar cycle projections were related to the GCR deceleration parameter, $\phi(t)$, which was correlated with neutron monitor data to represent the temporal GCR environment in interplanetary space. Future solar cycle activity levels up to the year 2020 were calculated using a statistical model for solar cycle projection, which was developed using the observed sunspot data (Kim and Wilson, 2000; Kim *et al.*, 2004, 2006; Wilson *et al.*, 1999). The odd and even cycles are treated separately because each possibly depends upon the orientation of the solar dipole moment, reversing between even and odd cycles (Hale 1908; Babcock 1961; Noyes 1982; Withbroe 1989). The projections of sunspot numbers in the rising and declining phases of a cycle were also made separately from two distinct correlation patterns (Wilson et al. 1999).

In interplanetary space, the constant flux of GCR outside of the Earth's magnetic field delivers a steady although low-level dose rate to astronauts. The variation of the GCR flux intensity over the approximately 11-year solar cycle, which is due to the interplanetary plasma resulting from the expanding solar corona, is shown as the GCR deceleration parameter in Fig. 1. The calculated value as a function of time allows us to project GCR environments into the near future.

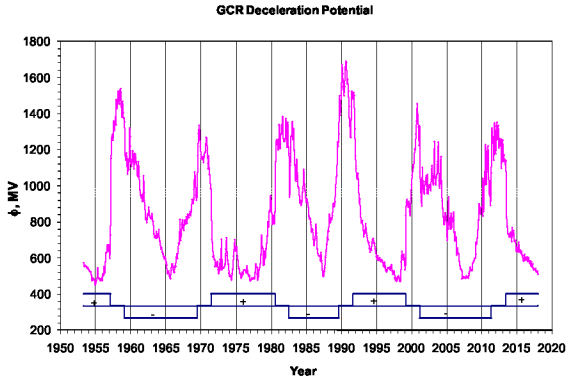

Fig. 1: GCR deceleration parameter as a function of time calculated from a statistical model.

The average GCR deceleration parameters for the possible mission durations of 6, 20, and 30 months are shown in Fig. 2, assuming the mission started at any given time in a solar cycle, and lasted for the successive months of a given mission duration. Since it is impossible to predict whether a future mission will take place in a cycle similar to any of previous solar cycles on record, the average values are combined to estimate an overall cumulative probability distribution in Fig 3, by which the percentile rank of the average interplanetary space radiation environment was represented for a given mission duration. The GCR energy spectra for all of the elements at a given distance from the Sun were derived from Badhwar and O'Neill's model (1992). In this model, a single input value of $\phi(t)$ describes the strength of the Sun's magnetic field with solar minimum at 428 MV and solar maximum at $\phi > 1{,}000$ MV.

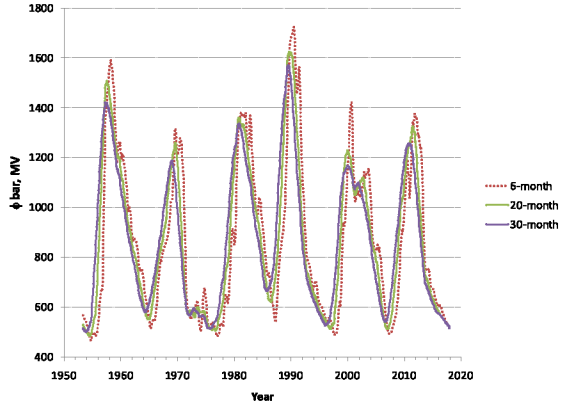

Fig. 2: The average GCR deceleration parameters, ϕ bar, for mission periods of 6, 20, and 30 months, as if a mission started at any time in a solar cycle and lasted for successive months of a given mission duration.

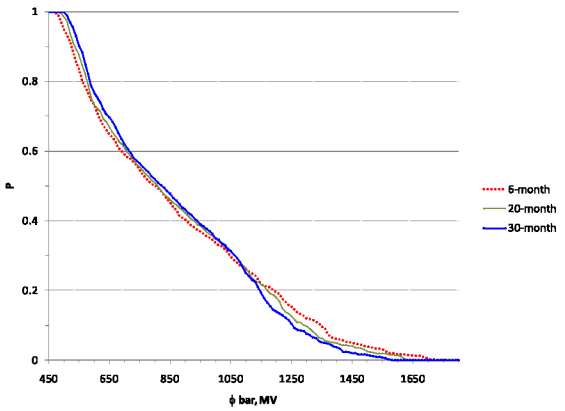

Fig. 3: Cumulative probability distribution of the average GCR deceleration parameters (using the same data in figure 2) for mission periods of 6, 20, and 30 months.

3.2 Prediction of SPE frequency for a non-specific future cycle

The 370 SPEs identified during solar cycles 19–23 varied significantly in the overall distribution of Φ_{30} from cycle to cycle. However, fluence data of Φ_{30} were combined over all 5 cycles to estimate an overall probability distribution of an average cycle. Fig. 4 shows sample cumulative probabilities of Φ_{30} for cycles 19-23 and the overall cumulative probability (thick line without centered symbol). Also included in Fig. 4 are the probabilities of the impulsive nitrate events of 71 SPEs with $\Phi_{30} > 2\times10^9$ protons cm^{-2} (McCracken et al. 2001) with and without seasonal correction, and they are not significantly different from the modern sets of large Φ_{30} data (Shea and Smart, 1990).

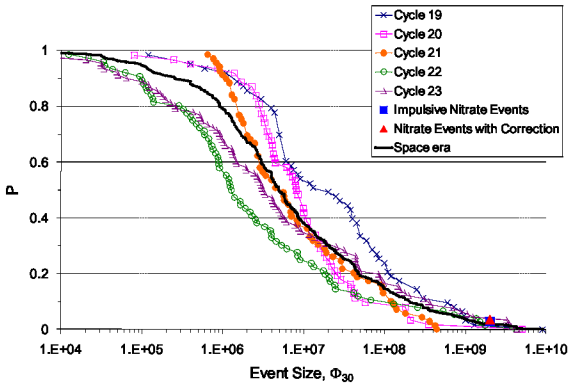

Fig. 4: Probability of an SPE event exceeding the displayed threshold Φ_{30} (combined data of space era is thick line; data for each cycle is a solid line with a centered symbol; impulsive nitrate events with and without seasonal correction have symbol only displayed).

While the expected frequency of SPEs is strongly influenced by the phase of the solar activity cycle, the SPE occurrences themselves are random in nature. The onset dates of a total of 370 SPEs during solar cycles 19–23 are marked in the top of Fig. 5 as brown vertical lines. More frequent SPE occurrences are shown as dense vertical lines, which are located typically near the middle of cycles. Large enough SPEs with proton fluencies at energy > 30 MeV, $\Phi_{30} > 1\times10^7$ protons cm^{-2}, are also shown in Fig. 5. Other than a general increase in SPE occurrence with increased solar activity, recent solar cycles have yielded no recognizable pattern of when and how large individual SPEs occur (Goswami et al. 1988; Kim et al. 2005). There have been several occurrences of intense SPEs during solar active years, which are typically 2.5 years before and 4.5 years after solar maximum. The data in Fig. 5 lead to the observation that individual SPE size is randomly distributed.

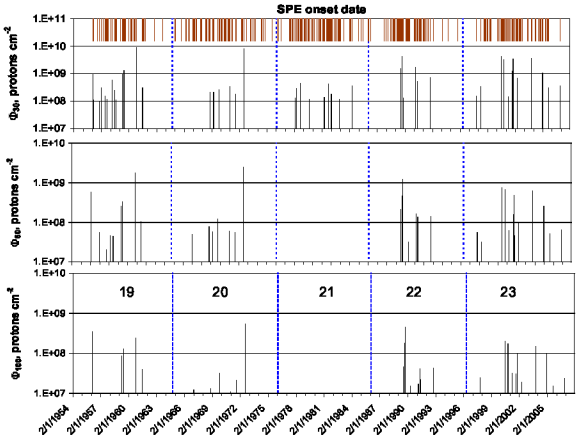

Fig. 5: SPE onset date marked as vertical lines in the top of the figure; and large SPEs recorded during 5 modern solar cycles having integral proton fluences of Φ_{30}, Φ_{60}, and $\Phi_{100} > 1\times10^7$ protons cm^{-2} for energies > 30, > 60, and > 100 MeV, respectively.

The integral fluences at high proton energies, Φ_{60} and Φ_{100}, for some recorded SPEs are not always available. For cycle 21, there are no recorded measurements of large SPEs at high energies, as seen in the middle and bottom of Fig. 5. Simply, those high energy particles might not exist at all in cycle 21, and the cycle was quiet compared to other cycles shown in Fig. 5. Indeed the SPEs in cycle 21 can be characterized as having 'soft spectra', i.e., those SPE for which the high energy portion of the spectrum falls off rapidly. With this limitation, data from 1986 to the present (solar cycles 22 and 23) were used for the simulation of distributions of Φ_{60} and Φ_{100} for a given mission period. In that way, the simulation of proton fluences at those energies would be the best

available and reliable estimations for the crew protection.

For the random nature of SPE occurrences and event sizes, a probabilistic approach of modeling was developed using the recorded SPE database of proton fluence measurements of Φ_{30} that have occurred during the past 5 solar cycles (Kim et al. 2009a). First, the expected number of SPEs for a given mission period was estimated from a non-homogeneous Poisson process model, for which a non-constant hazard function has been defined to represent the propensity of SPE occurrences in the space era. Then, the distribution of proton fluence for each event occurrence was simulated with a random draw from a Gamma distribution at three proton energies, > 30, > 60, and > 100 MeV. With an estimated frequency of SPEs, total fluences from multiple SPEs during a given mission period were defined, ranging from the 5th to 95th percentile.

4. Radiation transport codes and various dosimetric quantities

To predict the propagation and interaction of the nucleons and heavy ions passing through various media, the galactic cosmic ray transport code, HZETRN (Wilson *et al.*, 1995), and the Baryon transport code for SPE, BRYNTRN (Cucinotta *et al.*, 1994), are used. These codes include the transport of nucleons and high-energy heavy ions up to an atomic number Z of 28 for HZETRN, and high-energy light particles with atomic number $Z \leq 2$ as well as neutrons (n, p, d, t, h, and α) for BRYNTRN. These codes solve the fundamental Boltzmann transport equation. To evaluate the flux of particles of type j with energy E, the input database consists of the stopping power, the macroscopic total nuclear cross sections, and the differential nuclear-interaction cross sections. These data are compiled in BRYNTRN (Cucinotta *et al.*, 1994) and for HZETRN (Wilson, *et al.*, 1995) using QMSFRG (Cucinotta et al. 2006).

The absorbed dose is the energy deposited at a given location x by all particles. For human exposure, the dose-equivalent is defined by the quality factor Q, which relates the biological damage incurred from any ionizing radiation to the damage produced by γ-rays. In general, Q is a function of linear energy transfer (LET), which depends on both particle type and energy. For dose equivalent calculations, the quality factors used are those defined by the International Commission on Radiological Protection in 1990 (ICRP, 1991).

Organ dose and dose equivalent assessments at a specific anatomical location are calculated using the particle fluxes for given number of rays that traverse various media, such as spacecraft, equipment, the tissue equivalent material, and any other media on the path of the ray. Each separate medium's thickness distribution along a ray surrounding a specific organ at a specific position inside a spacecraft can be generated using the ray tracing model (Ponomarev et al. 2007; Nounu et al. 2009), which uses an evenly spaced distribution of the given number of rays over a 4π solid angle. For astronaut's organ dose and dose equivalent assessments, the human body geometry is based on the 50th percentile United States Air Force male/female in the standing position used by the Computerized Anatomical Man/Female model, CAM/CAF, respectively (Billings and Yucker, 1973). The effective dose, E, is defined as the sum of weighted equivalent doses over specified tissues and organs of the body. The organ dose equivalent is determined as an average of equivalent doses over all points in the organ or tissue, and the National Council for Radiological Protection (NCRP) adopted the organ dose equivalent as an acceptable approximation for equivalent dose for space radiation (NCRP, 2002). Therefore, the organ dose equivalents with the corresponding tissue/organ weighting factors, w_T (ICRP, 2007), were used for the approximation of the effective dose for stochastic effects from space radiation (NCRP, 2000, 2002).

For the deterministic acute effects, the quality factors for the dose equivalent generally overestimate the relative biological effectiveness (RBE), and NCRP (2000) has recommended that risks for non-cancer or deterministic effects be made in terms of an alternate dose quantity denoted as the Gray-Equivalent (Gy-Eq). This quantity uses radiation field dependent RBE for specific components, because distinct radiation quality functions occur for acute radiation risks and cancer. For the estimation of organ dose from space radiation, the new dosimetric quantity of Gray-Equivalent was implemented using the NCRP's RBE (2000) together with the suggested definition of neutron RBE (Wilson et al. 2002) for a full definition of total RBE. Table 1 show the RBE as given by NCRP and the suggested RBE values for neutron fields.

Particle type	RBE value	
	NCRP	Wilson *et al.*
<1 MeV neutrons	RBE (fission neutrons)	5.0
1-5 MeV neutrons	6.0	
5-50 MeV neutrons	3.5	
>25 MeV neutrons	RBE (not more than those of 1-25 MeV neutrons)	3.5
>2 MeV Protons	1.5	
Heavy ions (helium, carbon, neon, argon)	2.5	
Heavy ions, all others	2.5	

Table 1: Particle RBE (NCRP, 2000) and the RBE for neutrons suggested by Wilson et al. (2002) for deterministic effects.

5. Results and discussion

5.1 BFO dose assessment from large SPE exposure during interplanetary transit

For SPEs, the possibility of acute risk exists for a blood-forming organ (BFO) dose over 500 mGy-Eq. Such dose levels could occur from a SPE if the crew is in a thinly shielded spacecraft or during an EVA (Hu *et al.*, 2009). Dose limits for non-cancer radiation effects at BFO occur at doses below the threshold for prodromal effects. The current NASA 30-day limit is 250 mGy-Eq (NRC/NAS, 2008). The BFO dose was assessed with the full energy spectrum of historically large SPEs inside aluminum and polyethylene shielding materials with a spherical structure of 10 g/cm^2-thickness in Fig. 6a and b; and 15 g/cm^2-thickness in Fig. 7a and b. They are a function of proton fluence above energies greater than 100 MeV, Φ_{100}.

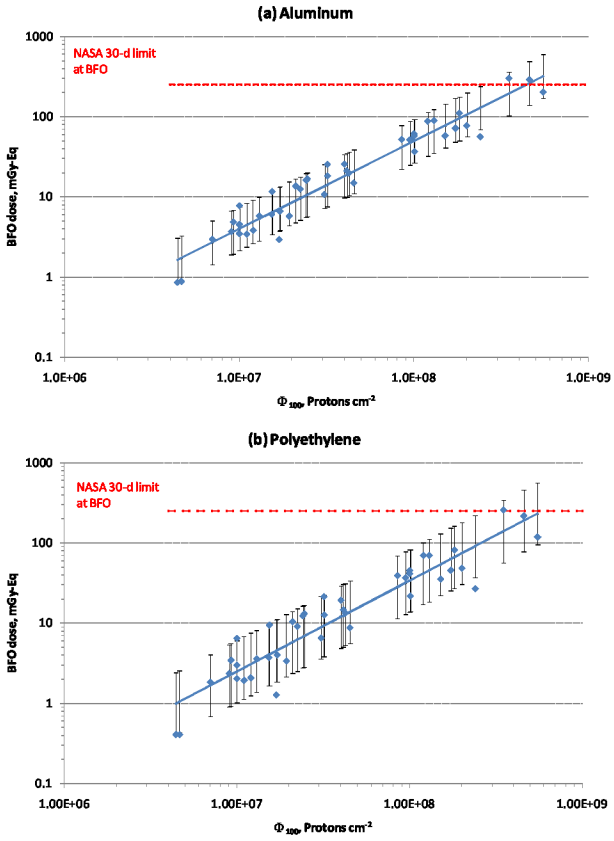

Fig. 6: BFO dose vs. Φ_{100} of historically large SPEs inside a 10 g/cm^2 of sphere in interplanetary space: (a) Aluminum and (b) polyethylene. The best linear fit regression line is shown, along with 90% tolerance limits. The current NASA 30-day limit at BFO is shown as the horizontal dashed line.

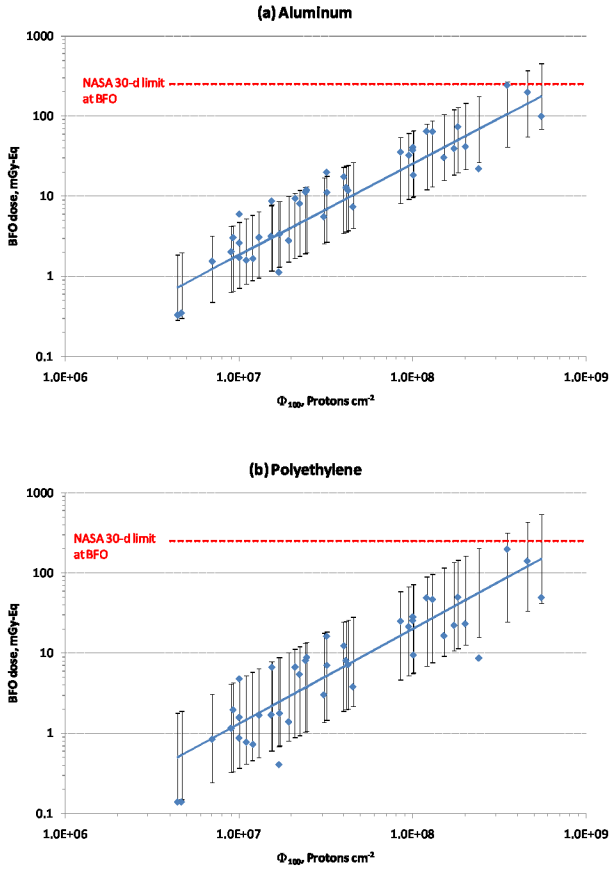

Fig. 7: BFO dose vs. Φ_{100} of historically large SPEs inside a 15 g/cm^2 of sphere in interplanetary space: (a) Aluminum and (b) polyethylene. The best linear fit regression line is shown, along with 90% tolerance limits. The current NASA 30-day limit at BFO is shown as the horizontal dashed line.

These data appear to be reasonably defined by a linear trend on a log-log scale, included as a solid line in the figures. The assumed Gaussian distribution of BFO dose around the regression line is attributable to variability of SPE energy spectra. Vertical lines represent a range from the 5th to the 95th percentiles of the distribution of BFO dose for future SPEs as a function of Φ_{100}. Included in the figure is the current NASA 30-day limit at the BFO (horizontal dashed line). Shielding effectiveness of polyethylene was compared to aluminum for BFO dose reduction. Polyethylene gave a reduction of 33 ± 11% and 39 ± 12% relative to aluminum at thicknesses of 10 and 15 g/cm^2, respectively.

Using this fitted regression model, the probabilities of exceeding the NASA 30-day limit of BFO dose for aluminum, water, and polyethylene were calculated as a function of Φ_{100}, and they are shown in Fig. 8. In case of a SPE with an excess of higher energy protons, the probability increases rapidly as a function of the integral fluence of Φ_{100} as illustrated

in Fig. 8. Risk assessment can be more directly determined by protons with higher energies (Kim et al. 2009b). Solar spectral forms based on the measurements of high energy protons beyond 100 MeV are critical to the accurate assessment of radiation risk from SPEs. From this, it is clear that the measurement of fluences of the high energy protons should become a requirement, in order to lower the false-alarm rate of a warning system.

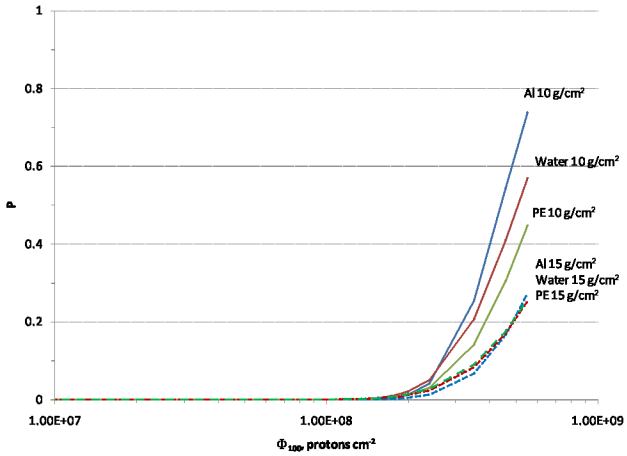

Fig. 8: Probability of exceeding the NASA 30-day limit of BFO dose for a given fluence level (Φ_{100} MeV) inside aluminum, water, and polyethylene of 10 and 15 g/cm^2 thicknesses in interplanetary space.

5.2 Effective dose analysis for rover design concept on lunar surface

Up to 15% of crew time may be spent in extra-vehicular activities (EVAs) on lunar missions. The major constraint for lunar surface mission is the time required to return to shelter for a short-term warning of SPE onset. A rover may be the only shelter in the worst case of being far away from a habitat. For the EVA strategy development considered by NASA, an administrative dose limit is set at 150 mSv for the rover design requirement to protect against a large 1972-type event. Fig. 9 shows the radiation dose analysis of a conceptual lunar rover from the August 1972 SPE. It shows the reduction of effective dose (E in mSv) by increasing cabin shell thickness to 5 g/cm^2 from the initial 0.8 g/cm^2 of aluminum to meet the design requirement for the configuration of 2 astronauts sitting in vertical orientation inside a rover. Greater reduction was achieved by adding 5 g/cm^2 of water-augmentation shielding inside a rover of 1 g/cm^2 cabin thickness. For the best protection, parametric optimization analysis should consider the astronauts' sitting orientation, multi-functional shielding materials, and lunar topology of lunar crater and cliff.

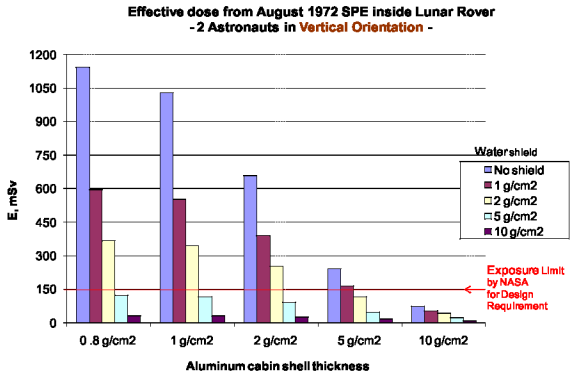

Fig. 9: Effective dose analysis of lunar rover concept with water shield augmentation for optimization of shield mass and effective dose reduction. NASA limit of 150 mSv for design requirement is shown as horizontal line.

5.3 Effective dose contribution by each charge group from GCR at solar minimum

Annual effective doses from GCR at solar minimum in interplanetary space (blue) for males are calculated in Fig. 10 for various charge groups inside a spacecraft of 5 g/cm^2 aluminum. In interplanetary space, the dose contribution of various GCR charge groups and their secondaries is considerable. These heavy nuclei are a concern for radiation risks, because they have the highest biological effectiveness and leave columns of damage at the molecular level as they traverse a biological system. A plausible mitigation method by shielding is impossible due to the high penetration power of energetic particles of GCR.

On the Martian surface, the interplanetary GCR fluxes at solar minimum were propagated through its atmosphere of 16 g/cm^2 carbon dioxide. The annual effective doses for males are shown in the same figure for the Martian surface (red) from GCR where radiation protection by Martian atmospheric shielding and the shadow effect of Mars itself was included. Also shown in the figure is the estimate of effective dose for males during a 30-month Mars mission (green), which includes interplanetary transit to/from Mars for 6-months each way, and a Mars surface stay for one and a half years. The total effective dose was estimated to be about 1 Sv for male crew members inside a 5 g/cm^2 of aluminum sphere at solar minimum.

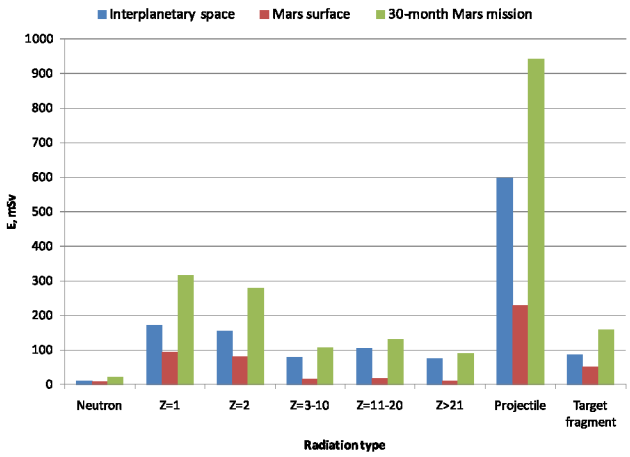

Fig. 10: Effective dose of each charge group, overall projectile of GCR, and target fragmentation inside a spherical spacecraft with 5 g/cm^2 aluminum: Annual exposure in interplanetary and on Mars surface; and that for 30-month Mars mission.

Career dose limits, which correspond to a 3% risk of cancer mortality for a 10 year career, are recommended by the National Council on Radiation Protection and Measurements (NCRP, 1989 and 2000) and are shown in Table 2. The estimation in Fig. 10 of effective dose for a 30-month Mars mission exceeded the career limit of a 35-year old male astronaut, (0.9 Sv of the NCRP limit (2000)). When a vehicle geometry and a Mars mission scenario are defined in detail, the probabilistic risk assessment would be made accurately for the protection of astronauts. By using various levels of particle intensities of the GCR environment as in Fig. 3, the range of risk can be assessed.

	NCRP Report No. 98 (Sv)		NCRP Report No. 132 (Sv)	
Age	Male	Female	Male	Female
25	1.5	1.0	0.7	0.4
35	2.5	1.75	0.9	0.6
45	3.25	2.5	1.5	0.9
55	4.0	3.0	2.9	1.6

Table 2: Career dose limits corresponding to 3% cancer mortality for 10 year careers as a function of age and sex. (NCRP, 1989 and 2000).

5.4 Probabilistic risk assessment for cancer mortality from space radiation

Lifetime cancer mortality described as risk of exposure induced death (REID) is employed by NASA as the quantity for setting age and gender specific career dose limits. Career exposure to radiation is limited by NASA as not to exceed 3% REID from fatal cancer. NASA policy is to assure that this risk limit is not exceeded at the 95% confidence level, using a statistical assessment of the uncertainties in the risk projection calculations to limit the cumulative effective dose received by an astronaut throughout his or her career. These limits are applicable to missions in low Earth orbit (LEO) of any duration and to lunar missions. Non-cancer mortality risks and approaches to reducing uncertainties in cancer risk projection models must be considered further for longer missions outside LEO. The whole body effective dose defined as a summation over radiation types and organ/tissues using the tissue weighting factors, w_T (ICRP, 2007), was calculated in Table 3 for inside a storm shelter of a conceptual lunar habitat from the exposure to the GCR and SPE for 180-day lunar mission. Based on the probabilistic risk assessment for a conceptual lunar habitat, we observed that the timeline for future long-term lunar and Mars missions would be preferably at solar maximum rather than at solar minimum, because the storm shelter for SPE was not effective for GCR exposure. A judiciary decision to add a well-shielded region inside the habitat as well as other medical treatments is required to lower the possibility of exceeding the acceptable level of 3% at the upper 95% confidence interval.

		Solar Minimum		Solar Maximum	
		Male	Female	Male	Female
Effective dose, mSv		152	152	72.1 (median) 157.1 (upper 95% CI)	72.6 (median) 155.5 (upper 95% CI)
Age, yr		%REID Carcinogenesis			
Median	35	0.58	0.72	0.28	0.35
	40	0.52	0.64	0.25	0.31
	45	0.45	0.54	0.22	0.26
	50	0.39	0.46	0.19	0.22
	55	0.33	0.39	0.16	0.19
Upper 95% CI	35	2.3	2.8	1.7	2.1
	40	2.1	2.5	1.6	1.9
	45	1.8	2.1	1.3	1.6
	50	1.5	1.8	1.2	1.4
	55	1.3	1.5	1.0	1.2

Table 3: %REID carcinogenesis for 180-d lunar mission at storm shelter inside a conceptual lunar habitat.

6. Concluding remarks

The future space radiation environment, including the GCR environment and the event-integrated fluence of SPEs, was estimated using the statistical models, which were developed according to the observed space databases. For the planning of future missions,

organ dose and dose equivalent, and effective doses were analyzed for various shield design specifications. The cancer risk assessments of a lunar mission with 95% confidence interval showed the age, gender, and solar cycle dependence from the risk projection models. It was concluded that future space missions should be launched at solar maximum rather than at solar minimum to minimize the possibility of exceeding the acceptable 3% REID at the upper 95% confidence interval. To protect crew members on a surface mission, the dose reduction below the exposure limit of 150 mSv for rover design requirement was achieved by augmented multi-functional shielding mass, i.e., water for life support, thermal control, and shielding.

Probabilistic risk assessment can be applied for the estimation of the effectiveness of the risk mitigation methods, including the candidate spacecraft designs and mission timelines, as well as the definition of the proper shielding requirements and identification of future exploration mission scenarios. The results can be applied to the development of approaches to improve radiation protection of astronauts and to the optimization of mission planning for future space missions.

For the probabilistic assessment of radiation risk from SPEs during a given mission period and a defined shielding configuration, the simulation must take into account not only the randomness of SPE occurrences and total proton fluence, but also the variation of energy spectra of the SPEs, because the detailed energy spectrum is the important parameter. Because there is a very limited theoretical basis for spectral fits to SPEs, the measurements of proton fluences at $E > 100$ MeV emitted during SPEs are required for an accurate risk assessment.

References

Babcock, H. W. The topology of the Sun's magnetic field and the 22-year cycle. *Astrophys. J.*, 133, no. 2, 572–587, 1961.

Badhwar, G. D., O'Neill, P. M., Improved model of galactic cosmic radiation for space exploration missions. *Nucl. Tracks & Rad. Meas.*, 20, no. 3, 403-410, 1992.

Badhwar, G. D., Cucinotta, F. A., O'Neill, P. M., An analysis of interplanetary space radiation exposure for various solar cycles. *Radiat. Res.*, 138, no. 2, 201-208, 1994.

Billings, M.P., Yucker, W.R. The computerized Anatomical Man (CAM) Model, NASA CR-134043, 1973.

Cucinotta, F.A., Wilson, J.W., Badavi, F.F. Extension to the BRYNTRN code to monoenergetic light ion beams. NASA TP-3472, 1994.

Cucinotta, F.A. Issues in risk assessment from solar particle events. *Radiat. Meas.*, 30, 261-268, 1999.

Cucinotta, F.A. and Durante, M. Cancer risk from exposure to galactic cosmic rays: implications for space exploration by human beings. *Lancet Oncol.*, 7, 431-435, 2006.

Cucinotta, F.A., Wilson, J.W., Saganti, P., Hu, X., Kim, M.Y., Cleghorn, T., Zeitlin, C., Tripathi, R.K. Isotopic dependence of GCR fluence behind shielding. *Radiat. Meas.*, 41, 1235-1249, 2006.

Durante, M., and Cucinotta, F.A., *Nature Rev. Cancer* (2008).

Eddy, J. A., The Maunder minimum. *Science*, 192, no. 4245, 1189-1202, 1976.

Goswami, J.N., McGuire, R.E., Reedy, R.C., Lal, D., Jha, R. Solar flare protons and alpha particles during the last three solar cycles. *J. Geophys. Res.* 93(A7), 7195-7205, 1988.

Hale, G. E. Magnetic field in Sun-spots. *Astrophys. J.*, 28, 315–343, 1908.

Hu, S., Kim, M.Y., McClellan, G.E., and Cucinotta, F.A., Modeling the Acute Health Effects of Astronauts from Exposure to Large Solar Particle Events, *Health Physics Journal*, 96(4), 465-476, April 2009.

ICRP, 1990 Recommendations of the International Commission on Radiological Protection. ICRP Publ. 60, Pergamon Press Inc., 1991.

ICRP Publication 103: The 2007 Recommendations of the International Commission on Radiological Protection, Annals of the ICRP, vol. 37/2-4, 2007.

Kim, M. Y., Wilson, J. W. Examination of solar cycle statistical model and new prediction of solar cycle 23. NASA/TP-2000-210536, 2000.

Kim, M. Y., Wilson, J. W., Cucinotta, F. A., An improved solar cycle statistical model for the projection of near future sunspot cycles. NASA/TP-2004-212070, 2004.

Kim, M.Y., Hu, X., Cucinotta, F.A. Effect of shielding materials from SPEs on the lunar and Mars surface, American Institute of Aeronautics and Astronautics, paper number AIAA 2005-6653, 2005.

Kim, M.Y., Cucinotta, F.A., Wilson, J.W. Mean occurrence frequency and temporal risk analysis of solar particle events. *Radiat. Meas.* 41, 1115-1122, 2006.

Kim, M.Y., Cucinotta, F.A., Wilson, J.W. A temporal forecast of radiation environments for future

space exploration missions. *Radiat. Environ. Biophys*. 46, 95-100, 2007.

Kim, M.Y., Hayat, M.J., Feiveson, A.H., Cucinotta, F.A. Prediction of frequency and exposure level of solar particle events, *Health Physics Journal*, 97(1), 68-81, July 2009a.

Kim, M.Y., Hayat, M.J., Feiveson, A.H., Cucinotta, F.A., "Using High-Energy Proton Fluence to Improve Risk Prediction for Consequences of Solar Particle Events," *Adv. in Space Res.*, doi:10.1016/j.asr.2009.07.028, 2009b.

Lopate, C., Simpson, J. A., The physics of cosmic ray modulation: heliospheric propagation during the 1987 minimum. *J. Geophys. Res.*, 96, no. A9, no. 15877-15898, 1991.

McCracken KG., Dreschhoff GAM, Zeller EJ, *et al.* (2001) Solar cosmic ray events for the period 1561-1994 1. Identification in polar ice, 1561-1950, *J. of Geophys. Res.,* 106, no. A10, 21585-21598

NCRP, *Guidance on Radiation Received in Space Activities*, NCRP Report No. 98., National Council on Radiation Protection and Measurements, Bethesda, MD, 1989.

NCRP, *Radiation Protection Guidance for Activities in Low-Earth Orbit.* Report No. 132, National Council on Radiation Protection and Measurements, Bethesda, MD, 2000.

NCRP, *Operational Radiation Safety Program for Astronauts in Low-Earth Orbit: A Basic Framework.* Report No. 142, National Council on Radiation Protection and Measurements, Bethesda, MD, 2002.

NRC/NAS, National Research Council/National Academy of Sciences, Committee on the Evaluation of Radiation Shielding for Space Exploration. Managing space radiation risk in the new era of space exploration, the National Academies Press; 2008.

Noyes, R. W., The Sun, Our Star. Harvard Univ. Press, Cambridge, MA, 1982.

Nymmik, R. A., Panasyuk, M. I., Suslov, A. A., Galactic cosmic ray flux simulation and prediction. *Adv. Space Res.*, 17(2), 19-30, 1996.

O'Neill, P., Badhwar–O'Neill galactic cosmic ray model update based on advanced composition explorer (ACE) energy spectra from 1997 to present, *Adv. Space Res.*, 37, 1727-1733, 2006.Ponomarev, A.L., Nounu, H.N., Hussein, H.F., Kim, M.Y., Atwell, W., and Cucinotta, F.A., NASA-developed ProE-based tool for the raytracing of spacecraft geometry to determine radiation doses and particle fluxes in habitable areas of spacecraft and in the human body, NASA/TP-2007-214770, 2007.

Shea, M.A. and Smart, D.F., A Summary of major proton events, *Solar Physics*, **127**, 297-320, 1990.

Wilson, J.W., Townsend, L.W., Nealy, J.E., Chun, S.Y., Hong, B.S., Buck, W.W., Lamkin, S.L., Ganapole, B.D., Kahn, F., Cucinotta, F.A. BRYNTRN: A Baryon transport model. Washington DC, NASA Report No. TP-2887, 1989.

Wilson, J.W., Townsend, L.W., Schimmerling, W., Khandelwal, G.S., Khan, F., Nealy, J.E., Cucinotta, F.A., Simonsen, L.C., Shinn, J.L., Norbury, J.W. Transport methods and interactions for space radiations. Washington DC, NASA Report No. RP 1257, 1991.

Wilson, J.W., Badave, F.F., Cucinotta, F.A., et al. HZETRN: Description of a free-space ion and nucleon transport and shielding computer program. NASA TP-3495, 1995.

Wilson, J. W., Kim, M. Y., Shinn, J. L., Tai, H., Cucinotta, F. A., Badhwar, G. D., Badavi, F. F., Atwell, W. Solar cycle variation and application to the space radiation environment. NASA/TP-1999-209369, 1999.

Wilson JW, Kim MY, De Angelis G, Cucinotta FA, Yoshizawa N, and Badavi FF. Implementation of Gy-Eq for deterministic effects limitation in shield design. *J. Radiat. Res.,* 43:S103-S106; 2002.

Withbroe, G. L. Solar activity cycle: history and predictions. *J. Spacecr. & Rockets*, 26, no. 6, 394–402, 1989.